

Zeitschrift: IABSE congress report = Rapport du congrès AIPC = IVBH
Kongressbericht

Band: 9 (1972)

Artikel: Dynamic design of high-rise building subjected to wind and seismic loads

Autor: Kawamura, Masayoshi / Wakabayashi, Kazuo / Ban, Shizuo

DOI: <https://doi.org/10.5169/seals-9607>

Nutzungsbedingungen

Die ETH-Bibliothek ist die Anbieterin der digitalisierten Zeitschriften auf E-Periodica. Sie besitzt keine Urheberrechte an den Zeitschriften und ist nicht verantwortlich für deren Inhalte. Die Rechte liegen in der Regel bei den Herausgebern beziehungsweise den externen Rechteinhabern. Das Veröffentlichen von Bildern in Print- und Online-Publikationen sowie auf Social Media-Kanälen oder Webseiten ist nur mit vorheriger Genehmigung der Rechteinhaber erlaubt. [Mehr erfahren](#)

Conditions d'utilisation

L'ETH Library est le fournisseur des revues numérisées. Elle ne détient aucun droit d'auteur sur les revues et n'est pas responsable de leur contenu. En règle générale, les droits sont détenus par les éditeurs ou les détenteurs de droits externes. La reproduction d'images dans des publications imprimées ou en ligne ainsi que sur des canaux de médias sociaux ou des sites web n'est autorisée qu'avec l'accord préalable des détenteurs des droits. [En savoir plus](#)

Terms of use

The ETH Library is the provider of the digitised journals. It does not own any copyrights to the journals and is not responsible for their content. The rights usually lie with the publishers or the external rights holders. Publishing images in print and online publications, as well as on social media channels or websites, is only permitted with the prior consent of the rights holders. [Find out more](#)

Download PDF: 09.08.2025

ETH-Bibliothek Zürich, E-Periodica, <https://www.e-periodica.ch>

Dynamic Design of High-Rise Building subjected to Wind and Seismic Loads

Projet d'une structure élevée soumise aux charges dynamiques du vent et des séismes

Entwurf eines Hochbaues unter Berücksichtigung von dynamischen Wind- und Erdbebenkräften

MASAYOSHI KAWAMURA

Eng. D., Struc. Engr.

Nikken Sekkei Ltd, Japan

KAZUO WAKABAYASHI

Struc. Engr.

SHIZUO BAN

Eng. D., Prof. Emeritus

Kyoto University, Japan

TAKUJI KOBORI

Eng. D., Prof.

1. Introduction

The structural design of a high-rise building should be based on the different design principle depending on whether the building should be designed for wind load only or for wind load together with the effect of destructive earthquake. If the former is just the case, the greater the lateral stiffness of the building, the better the building for structural safety, whereas in the latter case, the increased stiffness causes a greater storey shear force to act on the building during an earthquake and is therefore often undesirable.

In a high-rise building for which seismic load is under prime consideration, the design is characterized by design conditions necessary for such a building and by structural solutions pertinent to such design conditions. Of a number of solutions that can be considered for the foregoing problem, the case of the KTC Building (The Kobe, Commerce, Industry and Trade Center Building, Kobe, Japan) is reported in this paper. The structural design for this building was accomplished in October 1967 and its construction was completed in October 1969.

2. Outline of the KTC Building

The KTC Building structure consists of a perimeter composed of a framed tube structure and a core consisting of braced rigid frames. As a structural solution for such a centre-cored high-rise building, this system can offer a number of advantages both for structural and economical problems. Figs. 1 and 2 show the typical plan and section of the KTC Building.

A framed tube structure used in the perimeter of a high-rise building essentially results in a very narrow width available for doorways at the ground floor level, and this gives rise to a problem to which a proper solution must be given.



KTC BLDG. (Kobe, Japan)

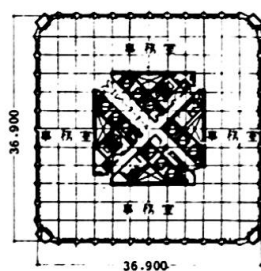


Fig.1 Typical plan

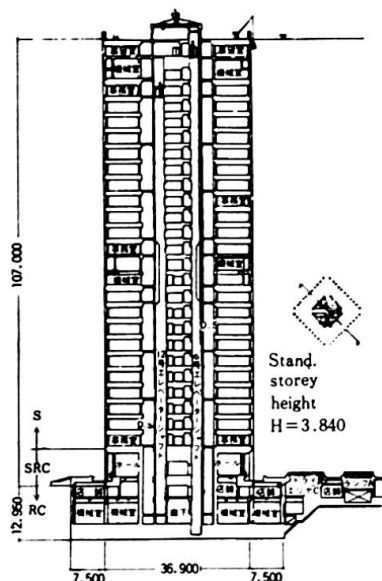


Fig.2 Section

In this building, the problem is solved by locating the main doorways at each corner of the perimeter where the column spacing is wider than elsewhere. This also makes it possible to carry out the column spacing on upper storeys down to the ground floor without modification of the continuous framework and is therefore considered an advantageous approach to the solution of this kind of problem. As a result of the foregoing doorway locations, the beams in the core structure are placed diagonally across the building, thereby serving to insure the horizontal rigidity of the core slab that has many through-floor opening space such as elevator shafts and stairways.

The structural system of this building is shown in Figs. 3 and 4. The structural design is featured by the following:

- a. The favourable minimum lateral stiffness of the building is given to resist wind force.
- b. The building is based on the dynamic design through the iteration of earthquake response analyses to resist seismic force.
- c. The structure is designed as a three-dimensional frame, consisting of the perimeter frame and cored frame, capable of resisting the foregoing lateral force.
- d. Efforts are made to give the framework continuity of stiffness, required strength and

sufficient ductility.

- e. The framework is designed in such a way that the yielding of members would occur in the beams and not in the columns or braces in the case of over-loading.
- f. The basement and the ground floor are constructed of the reinforced concrete and steel-frame reinforced concrete respectively to be sufficiently rigid so as to satisfy the assumption of the fixed base for the upper storey in the response analyses.
- g. The steel-frame reinforced concrete construction is adopted for the ground floor in order to avoid the abrupt stiffness change from the upper storeys to the basement.
- h. The steel construction is adopted for the second to the top floors so as to reduce the weight of the building structure. The qualities and thickness-to-width restrictions imposed on the principal members are given in Table 1.
- i. Both partitions and exterior walls are designed to minimize the weight of the building and also to be acceptable for such deflections as may be

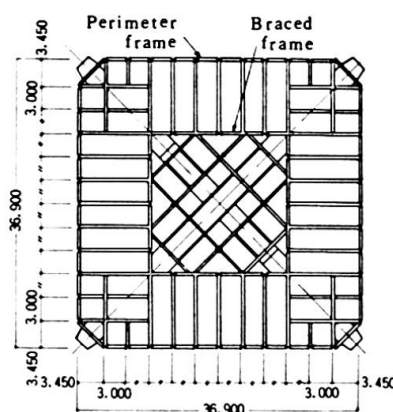


Fig.3 Beam plan

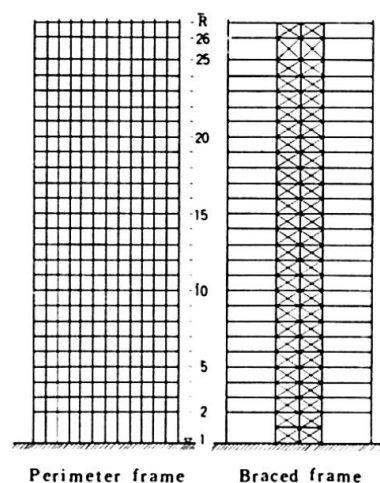


Fig.4 Structural system

caused during a great earthquake.

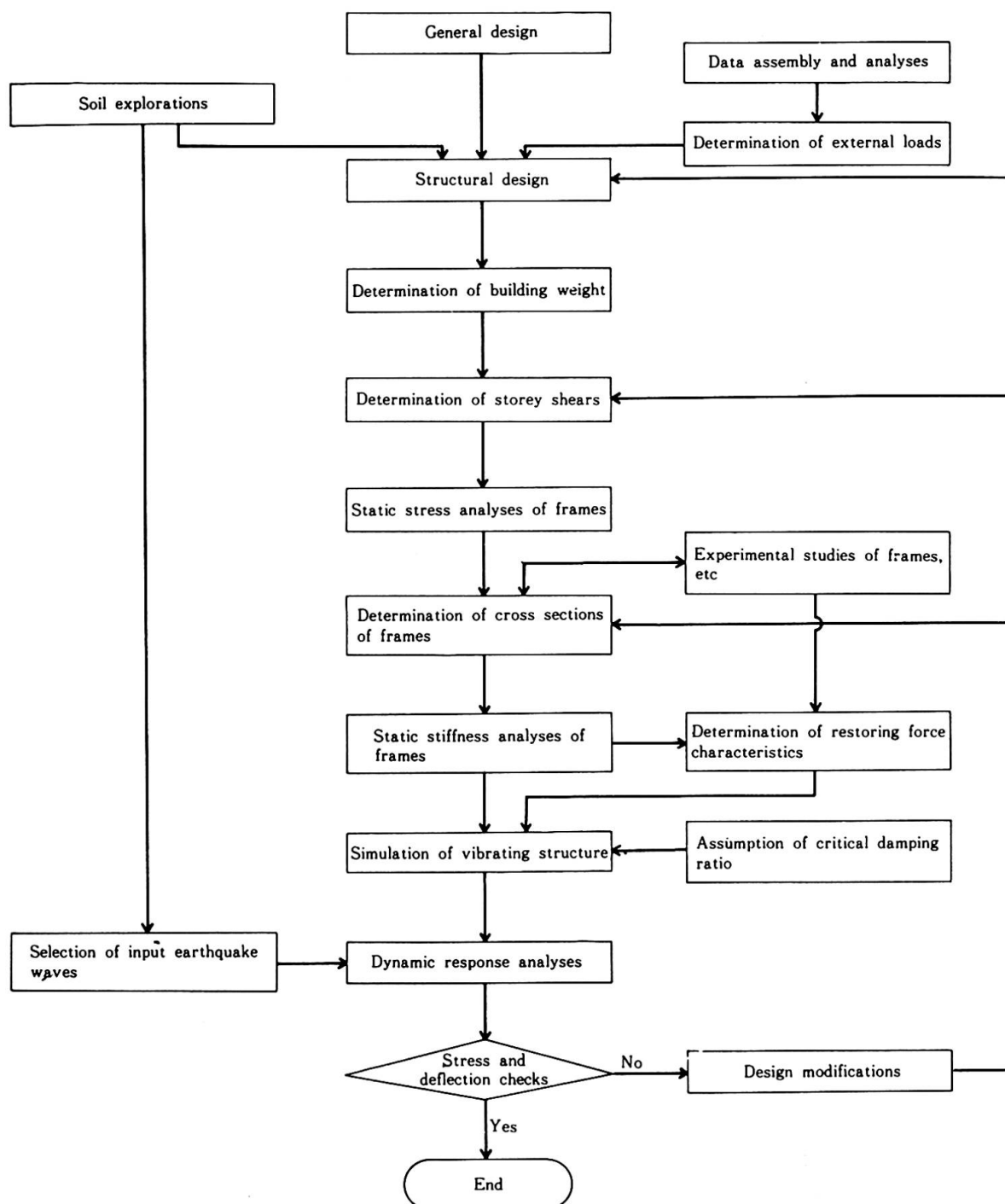
3. Aseismic Design

3.1 Design Procedure

The aseismic design procedure adopted for the KTC Building is as shown by the following chart:

Table 1 Materials

Member	Section	Quality	Max. b/t
Column	rolled H (series 400)	SM 50 A	flange 8
		SM 50 B	web 37
Beam (primary)	built-up H	SM 41	flange 9
			web 50
Beam (secondary)	built-up H rolled H honeycomb H	SM 41	flange 15
		SS 41	web 71
Brace	bar	Gr. 4	—



3.2 Basic Equation

The equation used in the dynamic analysis is written as follows:

$$[M]\{\ddot{y}\} + [C]\{\dot{y}\} + [K]\{y\} = -[M]\{\ddot{y}_0\}$$

where, $[M]$ = Mass matrix
 $[C]$ = Damping matrix
 $[K]$ = Stiffness matrix
 $\{y\}$ = Relative displacement vector
 $\{y_0\}$ = Ground displacement vector

3.3 Seismic Force and Permissible Storey Deflection

The input waves of earthquake ground motions adopted for this analysis are as shown in Figs. 14 and 15. As to the anticipated intensity of earthquakes, the maximum acceleration value of ground motions is estimated as 200 - 300 gals, because the maximum value of the greatest earthquake occurred in Kobe area was less than 100 gals in the past. Against these earthquake ground motions permissible deflection for each storey of the building is restricted to $h_i/200$ approximately (where h_i represents each storey height) so that stresses in all members would be within the elastic range. In addition, the elasto-plastic responses are analyzed with respect to earthquake motions with the maximum acceleration value of 400 gals. Since the natural period of a building often tends to be shorter than the computed period, the response characteristics are also studied in the case of the fundamental period which is assumed as 0.9 or 0.8 times the value of the computed natural period.

The seismic force used for the structural design is shown in Fig. 5. To evaluate this design seismic force, firstly the storey shears corresponding to the structural responses to the aforesaid ground motions are obtained through the iteration of response analyses for the case of the maximum acceleration value and the critical damping ratio assumed as 200 (300) gals and 2% respectively. Secondly, the storey shears thus obtained are plotted on a graph and an envelope embracing such plotted shears is evaluated finally as the applicable seismic force.

3.4 Wind Force and Permissible Storey Deflection

The design wind force to be assumed as a static external force is derived from the following formula:

$$P = C \cdot q \cdot A$$

where, C = Wind force coefficient
 (in this case, $C = 1.10$)
 q = Velocity pressure expressed as $q_0 \cdot \sqrt[4]{h/10}$ (in this case, $q_0 = 175 \text{ kg/m}^2$)
 A = Area exposed to wind force

In this formula, the value of q_0 is determined on the basis of the typhoons recorded in Kobe area in the past and the value of C , by a wind tunnel test of a model. The favourable minimum lateral stiffness of the building is determined in such a way that stresses in all the members would be within an elastic range, that the maximum deflection at the top of the building would not exceed $H/400$ (where H = the building height), and that the maximum storey deflection would be not

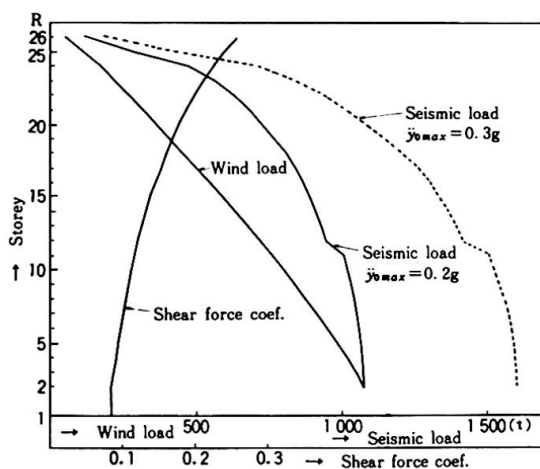


Fig. 5 Design loads

more than $h_i/300$ all under the foregoing wind force. The design wind force is shown in Fig. 5. The total wind force thus obtained is approximately equal to the base shear force caused by an earthquake ground motion where its acceleration value is taken as 200 gals.

3.5 Stiffness Distribution

The magnitude of earthquake response is governed by the characteristics of earthquakes and the dynamic properties (mainly dependent on mass and lateral stiffness distribution, i.e., natural periods and modes of vibration) of the building structure. While the structural engineer has little freedom in selecting the mass distribution, he can choose the desirable stiffness distribution more freely.

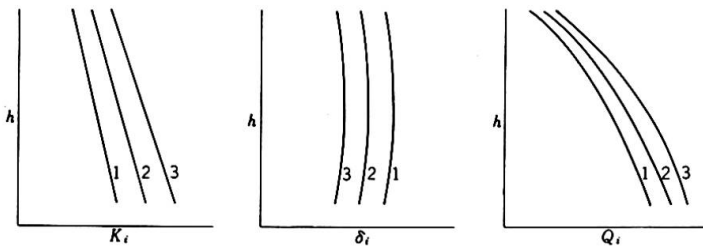


Fig. 6 General relationship between stiffness and response

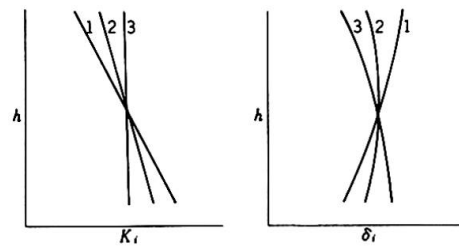


Fig. 7 General relationship between stiffness and storey deflection

In the first place, it may be stated that the shear force generally tends to increase as the stiffness of a structure increases (or in other words as its natural periods decrease). On the contrary, the shear force decreases as the stiffness becomes small or as the natural periods become great. In this case, however, the horizontal deflection of the building increases. Fig. 6 shows a general tendency of the relationship mentioned above.

Secondly, it is known that lateral stiffness distribution in direction of the height of a building affects deflection distribution in that building. Each storey deflection should be made as uniform as possible throughout the height of a building; however, the stiffness must be adequately distributed in direction of the height of a building in order to achieve this purpose satisfactorily. Fig. 7 shows the general tendency of this relationship.

It is pointed out that the aseismic design requirement for a structure remarkably differs from the ordinary lateral force design as shown in Figs. 6 and 7. For instance, a heavily braced frame increases the stiffness of a building and enables it to favourably resist overturning moment at a reasonable cost, and is, therefore, satisfactory for a wind-resistant structure. Such a frame, however, often turns out to be undesirable for an earthquake-resistant structure, because it usually gives a building too large stiffness distributed as shown in curve 1 of Fig. 7.

In the structural design of the KTC Building, high strength steel bars are used for bracings. The purpose of such bracings is to optimize the stiffness distribution in direction of the height without increasing adversely the

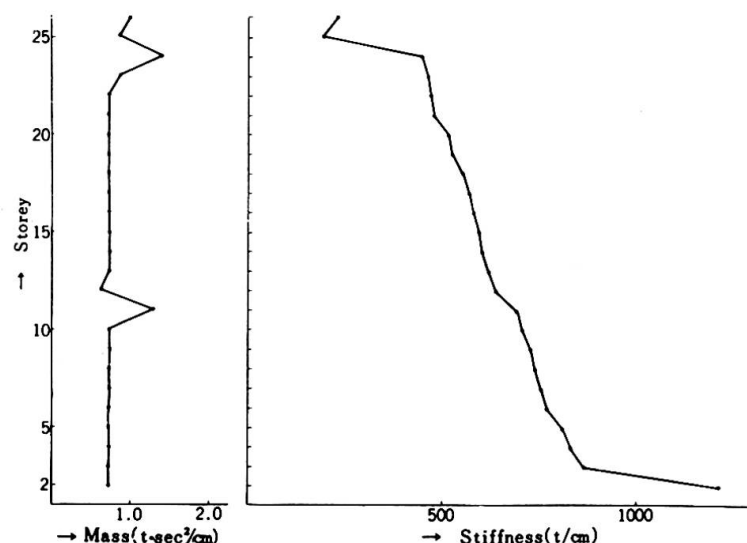


Fig. 8 Mass and stiffness distribution

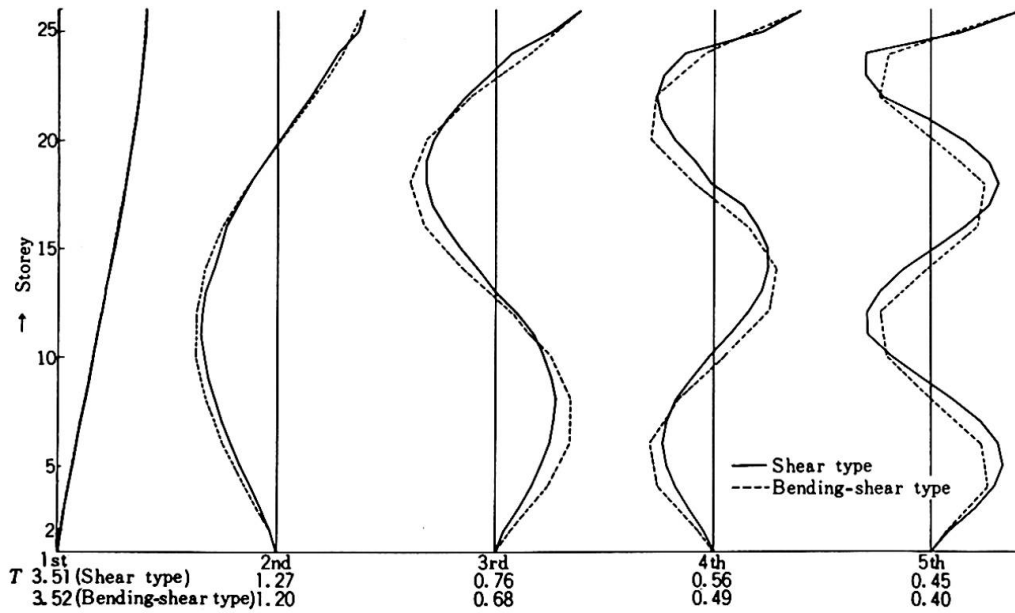


Fig. 9 Modes of vibrations and natural periods

stiffness of the building as a whole and to sufficiently enlarge the elastic range of the bracings. These braces are capable of deforming within an elastic range under a storey deflection up to 4 cm approximately.

Fig. 8 shows the mass distribution and the stiffness distribution (under the shear type vibration) as computed for a simulated model of the KTC Building idealized by the lumped mass system. The earthquake responses of such a model are shown in Figs. 11 through 13. The stiffness distribution as shown in Fig. 8 ensures the response deflection which is approximately made uniform through all storeys within an allowable limit. Table 2 shows the computed natural periods for the building as completed (without live loads) and for the building as occupied (with live loads). Fig. 9 shows each mode of vibration to which the building under occupancy would be subjected.

3.6 Results of Analyses

Some results of the earthquake responses analyses are shown in Figs. 11 - 14. Fig. 11 indicates the vibration of simulated model of the building idealized

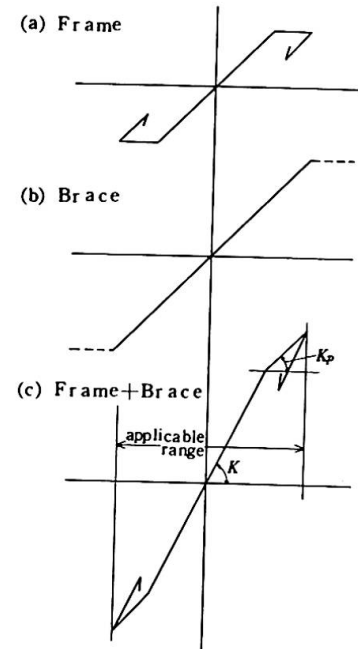


Fig. 10 Elasto-plastic restoring force characteristic

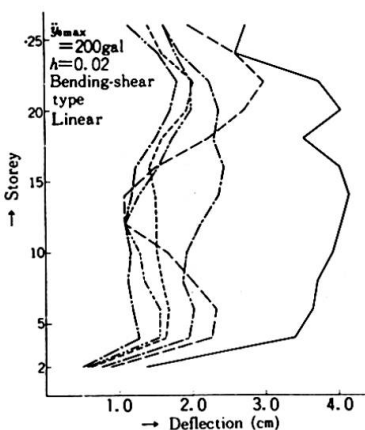


Fig. 12 Deflection in earthquake response

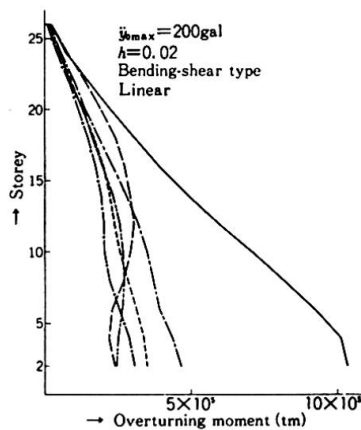


Fig. 13 Max. overturning moment in earthquake response

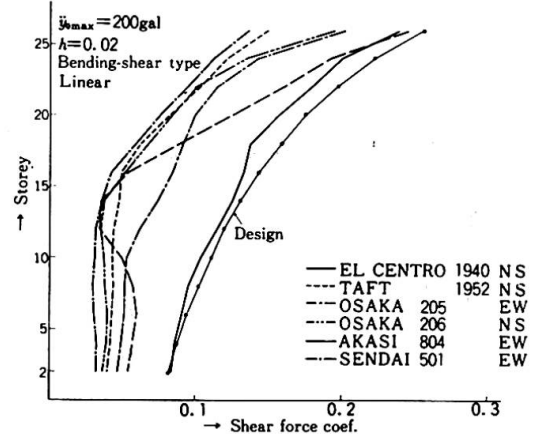


Fig. 14 Max. shear force coef. in earthquake response

Table 2 Natural periods

Vibration type	Assumed condition	T	T	T	T	T
Shear type	Before occupancy	3.51	1.27	0.76	0.56	0.45
Bending-shear type	Before occupancy	3.52	1.20	0.68	0.49	0.40
	After occupancy	3.33	1.14	0.64	0.46	0.37

shear force coefficient computed from earthquake responses. The ductility factors corresponding to various input earthquake waves are shown in Fig. 15. In these analyses, every two storeys are considered one lumped mass except for Fig. 11 in which each storey is considered one lumped mass.

The elasto-plastic restoring force characteristics of the framework are assumed, as a whole, to be bi-linear as shown in Fig. 10. From these results, it is known that the earthquake responses largely depend on the patterns of input earthquake waves. The maximum storey deflection is within $h/200 - h/250$, the permissible deflection range, under the maximum acceleration amplitude of 200 gals of input waves. Some portions of the frame structure are in a plastic range under El Centro 1940 (NS component) of the maximum acceleration amplitude in excess of 300 gals. However, the ductility factors are not more than 1.2 and 2.0 under the maximum acceleration values of 300 gals and 400 gals respectively. In studies with regard to the other wave patterns it is found that the responses remain in elastic range under the maximum acceleration amplitude of about 500 gals.

The results of wind load analysis as shown in Table 3 indicate that the storey deflection at lower storeys is about $h/320$ or about 40% of the maximum deformation in an elastic range. The maximum deflection at the top of the building is approximately $h/460$ corresponding to the sufficient stiffness of the frame against the wind load.

by the lumped mass system as related to time lapse during earthquakes. Figs. 12 and 13 show the deflection and the maximum overturning moment in earthquake responses respectively. Fig. 14 indicates the maximum

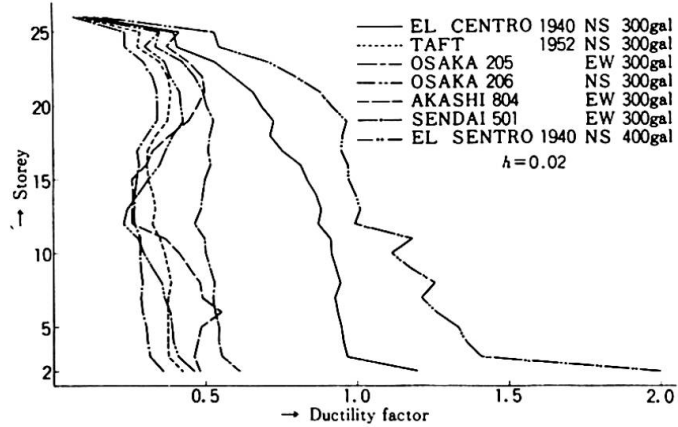


Fig. 15 Distribution of ductility factor

Table 3 Strength and stiffness under wind load

Storey	Storey shear (t)	Stiffness for wind load $K=(t/cm)$	Max-deflection in elastic range δ_{yi} (cm)	Max-storey deflection δ_i (cm)	h/δ_i	δ_i/δ_{yi}
26	46.6	186.4	9.70	0.25	1540	0.03
25	109.1	170.5	6.94	0.64	900	0.09
24	170.6	370.9	4.60	0.46	830	0.10
23	219.2	405.9	4.14	0.54	710	0.13
22	267.3	431.1	4.04	0.62	620	0.15
21	314.8	449.7	3.94	0.70	550	0.18
20	361.8	488.9	3.74	0.74	520	0.20
19	408.3	510.4	3.62	0.80	480	0.22
18	454.2	540.7	3.65	0.84	460	0.23
17	499.5	561.2	3.61	0.89	430	0.25
16	544.2	572.8	3.56	0.95	400	0.27
15	588.2	594.1	3.59	0.99	390	0.28
14	631.4	607.1	3.55	1.04	370	0.29
13	673.8	623.9	3.52	1.08	360	0.31
12	715.5	650.5	3.53	1.10	350	0.31
11	756.5	694.0	3.29	1.09	350	0.33
10	796.6	717.7	3.26	1.11	350	0.34
9	835.7	739.6	3.18	1.12	340	0.36
8	873.8	753.3	3.10	1.16	330	0.37
7	910.8	765.4	3.13	1.19	320	0.38
6	946.5	782.2	3.07	1.21	320	0.39
5	980.8	824.2	2.92	1.19	320	0.41
4	1,013.7	844.8	2.89	1.20	320	0.42
3	1,044.8	870.7	2.78	1.20	320	0.43
2	1,073.8	1,234	1.81	0.87	440	0.48

$$\delta_{top} = \sum \delta_i = 22.83 \text{ cm} \approx H/460$$

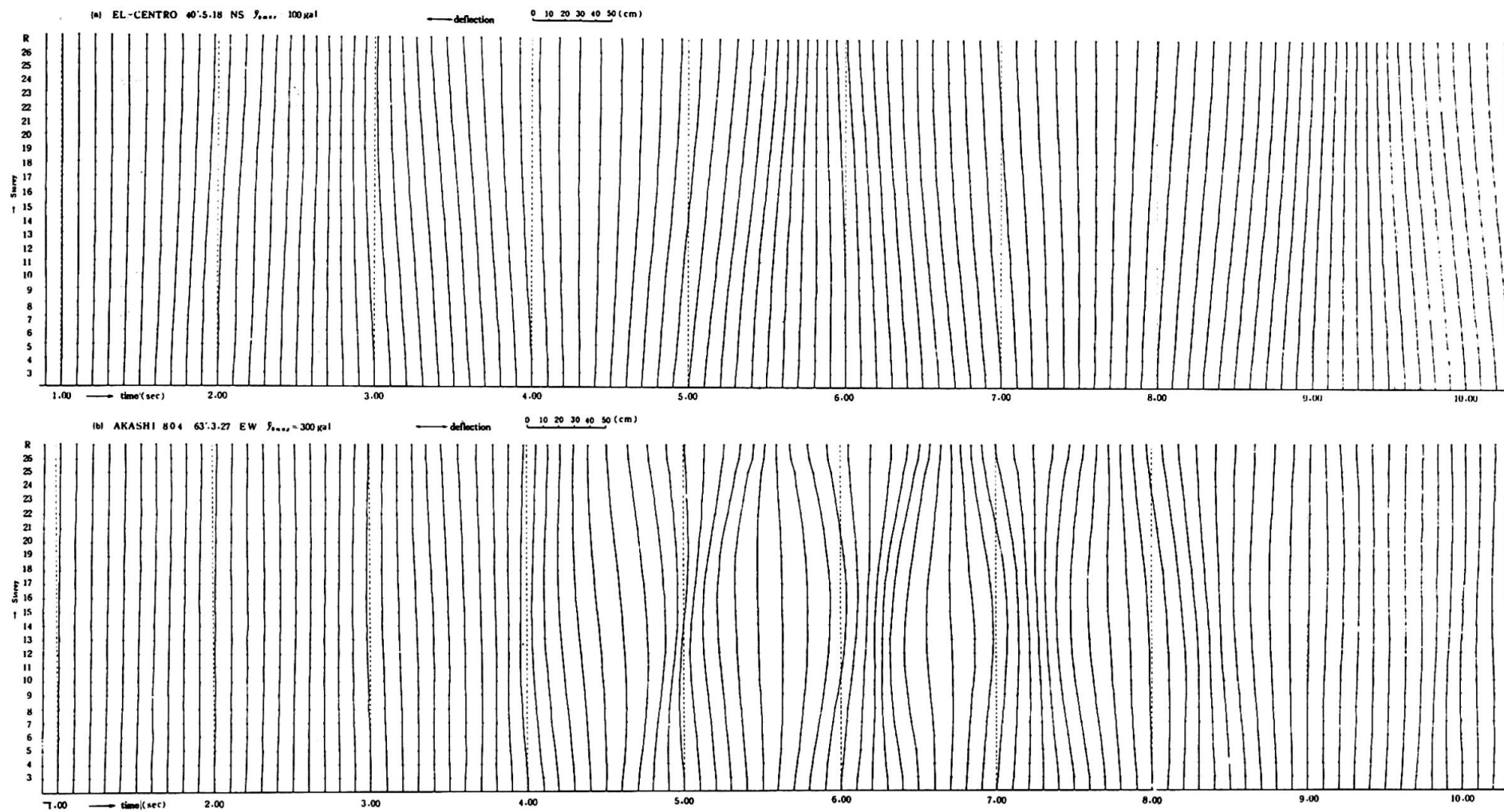


Fig. 11 Simulated vibration of the building

4. Vibration Tests

4.1 Test Procedure

When the building was under construction, its vibration characteristics were ascertained by such experimental approaches as forced vibration tests and micro-tremor measurements, and these experimental results were compared with the dynamic characteristics computed by means of theoretical analyses. The vibration tests consisted of the preliminary and main tests, and the main tests were carried out twice, first upon the completion of the framework and the second when the exterior and interior wall coverings had been placed.

For these tests, the excitation was effected by means of a pendulum and an oscillator located at the centre of the core. The excited storeys are shown in Table 4. The excitation by pendulum was intended to generate the fundamental mode of vibration, and for this purpose, a pendulum weighing 5 tons was suspended from the beams of the 25th floor. The oscillator was of eccentric mass type with maximum excitation capacity for 2 tons, and it was used to generate the 2nd to 5th modes of vibration of the building.

Table 4 Excitation procedures and excited storeys

Test	Procedures	E - W direction		N - S direction	
		${}_1T$	${}_2T \sim {}_5T$	${}_1T$	${}_2T \sim {}_5T$
Preliminary test	Micro-tremors				
1st and 2nd test	Micro-tremors				
	By pendulum By oscillator	25 F	26 F, 14 F	25 F	26 F

4.2 Test Results

Table 5 shows some of test results. As can be seen from the table, the measured values of the natural periods are about 75% of those obtained through theoretical analysis.

The measured natural periods obtained under micro-tremors coincide considerably well with those recorded under forced vibration. In this case the critical damping ratio does not exceed 1% under lower order vibrations of the building.

4.3 Discussion

The difference between theoretical and measured values of natural periods is largely attributable to the fact that the stiffness of the structure is evaluated on a different basis. In this connection, the following findings are made:

- (1) As high strength steel bars are slightly pre-tensioned, the bracings on compression side as well as tension side can contribute to the stiffness

Table 5 Results of vibration test

Tests	Natural periods		${}_1T$	${}_2T$	${}_3T$	${}_4T$	${}_5T$
Preliminary test	Computed values		T 2.21	0.80	0.49	0.35	0.27
	Measured values	Micro-tremors	T 1.73	0.65	0.40	0.28	0.21
1st test	Computed values		T 3.04	1.08	0.62	0.44	0.35
		*	T' 2.77	0.93	0.52	0.37	0.30
	Measured values	Micro-tremors	T 2.25	0.80	0.44	0.32	0.25
		Forced vibration	T 2.26 λ 0.50	0.80 0.53	0.45 0.95	0.32 1.80	0.25 2.20
2nd test	Computed values		T 3.33	1.14	0.64	0.46	0.37
		*	T' 3.04	0.97	0.54	0.39	0.31
	Measured values	Forced vibration	T 2.51 λ 0.87	0.82 1.28	0.43 2.40	0.31 2.1	0.22 2.9

* T' : modified values as mentioned in (4.3)

of the building under the small amplitude of vibration.

- (2) Concrete floor slabs are integrated with beams by means of stud connectors to produce composite effects.
- (3) Splice plates used for field connections of beams and columns increase the effective stiffness of the members concerned.
- (4) Gussets for brace connection help expand the zone of stiffness under bending moments.
- (5) No analysis is made as to the framework at the central core, located at an angle of 45° with respect to the principal frames, comprising four columns because its influence on the building stiffness is very small.
- (6) Exterior and interior walls are so detailed as to be separated from the principal structural frames; however, it is easily considered that they contribute to the stiffness of the building under small amplitude of vibration.

Of the foregoing findings, effects described in Subparagraphs (1) through (5) are taken into consideration and then the natural periods are re-computed accordingly. The modified values thus obtained are shown in Table 5. The ratio of the measured values to the modified values is about 82%, which is considered to be very satisfactory when compared with the difference between theoretical and measured values for similar experiments in the past. In making structural analyses of high-rise construction, the effects as described above must be considered.

Bibliography

- (1) Leonhardt, F. : High-Rise Slender Building : Introductory Report, 9th Congr. IABSE, Amsterdam 1972, pp. 233-237.
- (2) Wakabayashi, K., Kawamura, M., Ban, S., Yamada, M. : Bracing System composed of High-Strength Steel Bars as adopted in Aseismic Design of a High-Rise Building : Preliminary Publication, 9th Congr. IABSE, Amsterdam 1972.
- (3) Khan, F. R. : Column-Free Box-Type Framing with and without Core : Preliminary Publication, 8th Congr. IABSE, New York, 1968, pp. 261-273.
- (4) Ban, S., Kobori, T., Yamada, M., Kawamura, M., Wakabayashi, K. : Researches on the Structural Design of the KTC BLDG. : Annual Convention of the Architectural Institute of Japan, August 1969, pp. 1105-1118.

Summary

In the structural design of high-rise building, lateral stiffness of framework and its distribution in direction of the height of building must be given an essential consideration because the earthquake response characteristics of the building are greatly affected by these two important stiffness assessments. In stiffness computation, every computable factor which affects the structural behaviours should be taken into consideration.

A structural system consisting of rigid perimeter frames as well as of frames braced by high strength steel, so designed as to form a three-dimensional space structure, is believed to offer highly effective solution for the structural safety.